Conductivity of Gadolinium (III) Oxide (Gd_2O_3) in Hydrogen-containing Atmospheres

M. Khalid Hossain
Department of Advanced Energy Engineering Science, Interdisciplinary Graduate School of Engineering Science, Kyushu University

Kawaguchi, Kaname
Department of Advanced Energy Engineering Science, Interdisciplinary Graduate School of Engineering Science, Kyushu University

Hashizume, Kenichi
Department of Advanced Energy Engineering Science, Interdisciplinary Graduate School of Engineering Science, Kyushu University

Conductivity of Gadolinium (III) Oxide (Gd₂O₃) in Hydrogen-containing Atmospheres

*M. Khalid Hossain[1,2], Kaname Kawaguchi[1], Kenichi Hashizume[1]

[1]Department of Advanced Energy Engineering Science, Interdisciplinary Graduate School of Engineering Science, Kyushu University, Kasuga, Fukuoka 816-8580, Japan,

[2]Atomic Energy Research Establishment, Bangladesh Atomic Energy Commission, Dhaka 1349, Bangladesh.

*Corresponding author email: khalid.baec@gmail.com, khalid@kyudai.jp

ABSTRACT: *In this study, Gd_2O_3 was used to investigate the conductivity in H_2O and D_2O mixed with argon (Ar) atmospheres, and also in pure Ar and oxygen atmospheres ranging from 773 K to 1373 K to understand its possible application in the fusion reactor's tritium permeation barrier and purification system. The investigation shows that the conductivity of Gd_2O_3 is higher in both hydrogen-containing Ar atmospheres ($Ar+ H_2O$ and $Ar+D_2O$) than that in pure Ar. The obtained proton conductivity of Gd_2O_3 was about two orders lower in magnitude than that of a typical proton conductor $CaZr_{0.9}In_{0.1}O_3$ [1]. Therefore, Gd_2O_3 could be a potential material, but much improvement is required for the tritium recovery and purification system of nuclear fusion reactors.*

Keywords: Proton conducting oxides, Gd_2O_3, isotope effect, tritium recovery and purification, fusion reactor materials.

1. INTRODUCTION

Deuterium and tritium are used as fuel for nuclear fusion reactors [2]. From the viewpoint of safety and fuel loss of the fusion reactors, it is necessary to prevent the leakage of deuterium and tritium [3,4]. Therefore, it has been studied to use materials that do not readily pass hydrogen and could be suitable for the coating of metal piping in a fusion reactor for the tritium permeation barrier (Fig. 1(a)) [5–7]. It is also necessary to find materials through which hydrogen isotopes selectively pass through and purify the unused deuterium and tritium in fusion reaction [8,9]. Fig. 1(b) shows a conceptual diagram of tritium's purification system for a fusion reactor. T_2 is supplied to the fusion reactor, and neutrons (n) generated by the fusion reaction are reacted with lithium oxide (Li_2O). Then, by using a proton conductive oxide from the generated T_2, T_2O, He, and O_2, only T_2 is permeated and resupplied to the fusion reactor [10].

The application of proton conductive oxides to fuel recovery analysis and production systems is being
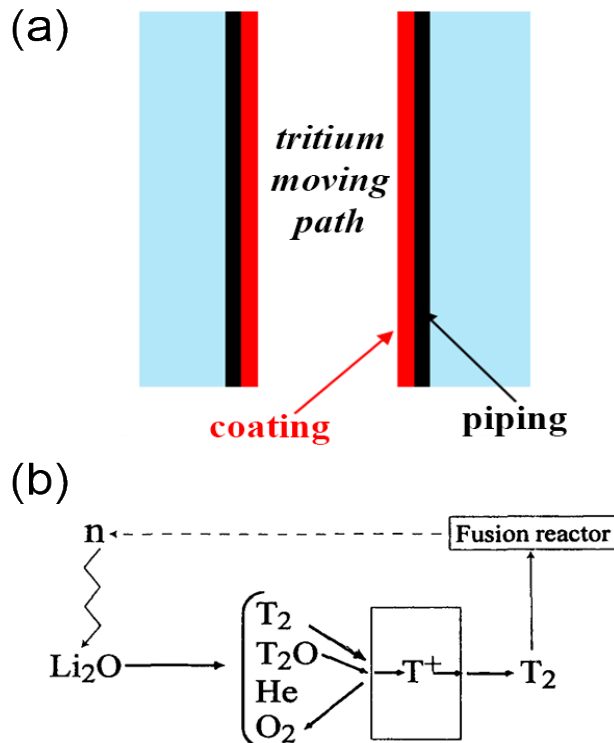

Fig. 1. Schematic diagram of (a) coating in inside the pipe of the tritium moving path, and (b) tritium purification system of a fusion reactor. Reprinted from Ref. [10].

studied by researchers [7,11,12]. It is known that oxide materials have the property to dissolve the hydrogen inside it and the diffusion coefficient is very small so that they can be used to prevent hydrogen permeation and leakage. Since some rare earth oxides have a small amount of dissolved hydrogen and are impermeable to hydrogen, they have been studied as candidates for this tritium leakage prevention coating material [6,7]. In actual use, even if the amount of dissolved hydrogen and the diffusion coefficient is low, if the amount used is large, the total amount of dissolution increases and it cannot be said that the hydrogen isotope tritium is not accumulated. At present, the amount of accumulated hydrogen such as the amount of dissolved hydrogen and the diffusion coefficient of each rare earth oxide is insufficient.

Lattice constants and crystal structures are considered to be factors that make hydrogen easier to dissolve in proton conductive oxides, and the relationship between hydrogen and oxygen diffusion is also considered [13]. Our previous studies reveal that rare earth oxides with a monoclinic crystal structure can easily dissolve hydrogen, and gadolinium oxide (Gd_2O_3) provides higher hydrogen solubility and diffusivity among seven rare-earth oxides at high-temperature atmospheres [11]. Therefore, Gd_2O_3 could be expected as a proton conductive material to purify and recover the unused deuterium and tritium in the fusion reactor's fuel cycle.

In this study, we measured monoclinic gadolinia's conductivity, which was easy to dissolve hydrogen, and investigated the conductivity of gadolinia in hydrogen, deuterium, and oxygen atmospheres.

2. EXPERIMENTAL

2.1 Sample preparation

After gadolinia powder was molded using a die press and cold isostatic pressure (200 MPa), it was heated in air at 1650 °C for 20 h to obtain the sintered sample [11,14,15].

2.2 Sample crystal phase identification by XRD
The crystal structure of gadolinia powder and sintered body were analyzed using Rigaku Corporation powder X-ray diffractometer XRD (MultiFlex) at the Central Analysis Center of Kyushu University. The crystal structure of the sample was identified from the obtained peak. The measurement conditions were a tube current of 40 mA, a 40 kV voltage, a scan speed of 4 ° / sec, and a light-receiving slit of 0.15 mm. The sample's crystal structure changed when the sample was changed from powder to a sintered body was examined using XRD.

2.3 Density measurement of sintered body sample
The apparent density and the relative density (apparent density with respect to the theoretical density) of the obtained sintered body sample were obtained by using the Archimedes method. The apparent density is determined by the following Eq. (1).

$$\rho_s = \frac{W_{dry}}{W_{wet} - W_{dry}} \times D_w \quad (1)$$

Here, Wdry and Wwet are the dry weight and underwater weight of the sample, respectively, and Dw is water density. The dry weight is the weight of the sample taken out of the furnace after sintering. After leaving it for a minute and taking it out, it was suspended in water to obtain a measured weight. An electronic balance (AUY220, manufactured by Shimadzu Corporation) was used for weight measurement.

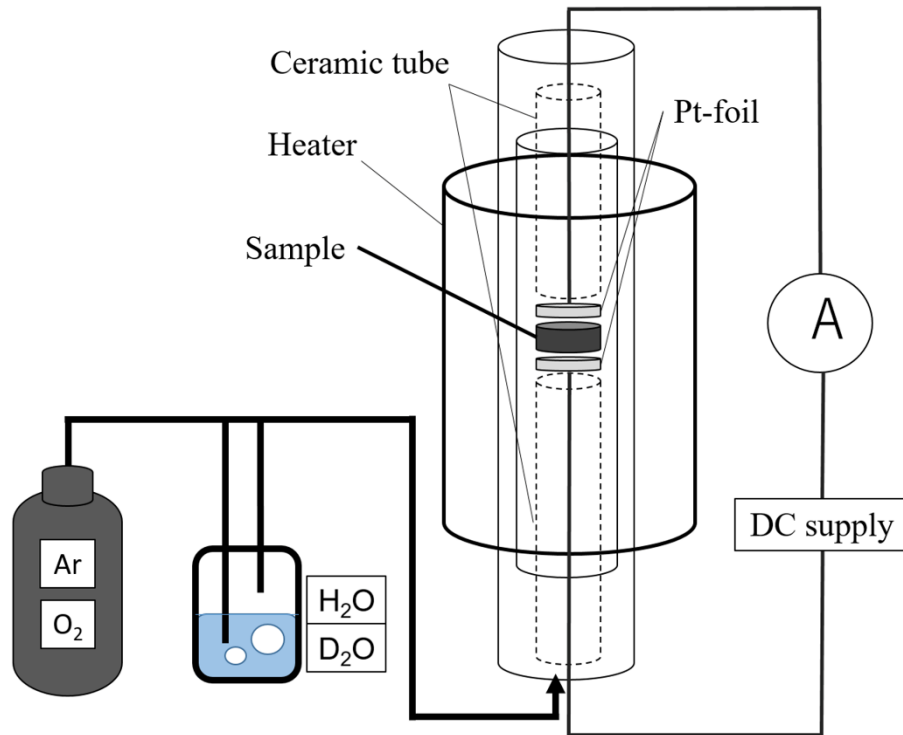### 2.4 Gadolinia conductivity measurement

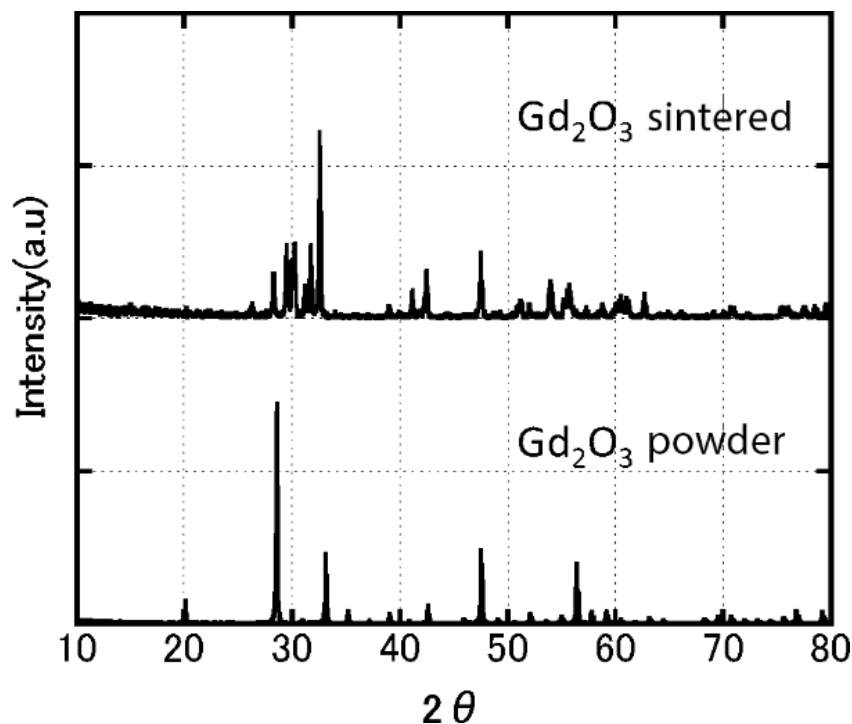Fig. 2. Schematic diagram of conductivity measuring device.

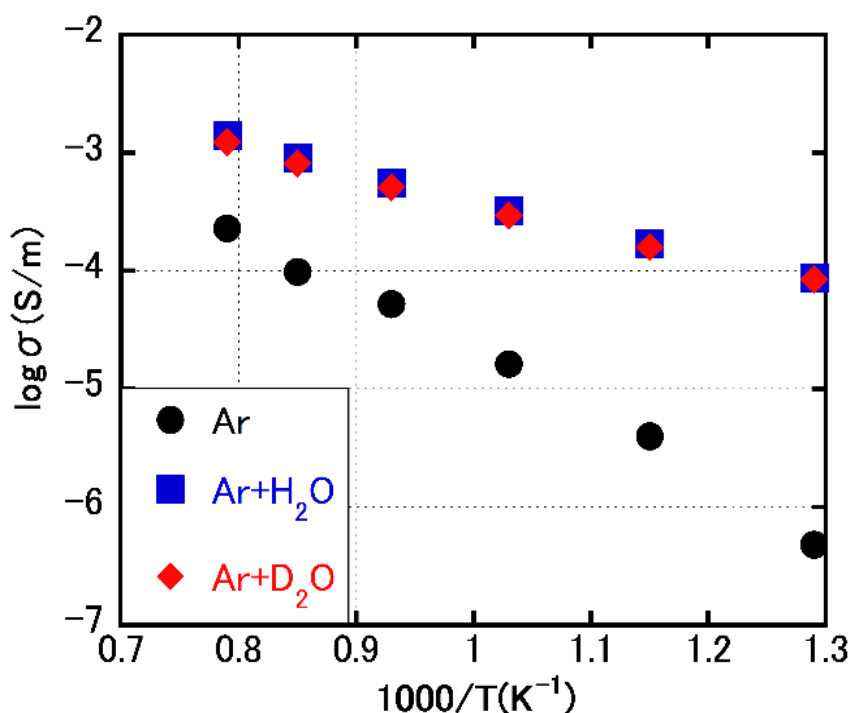Fig. 3. XRD results of powder and sintered gadolinia.

Fig. 4. Arrhenius plot of conductivity in Ar, Ar + H_2O, Ar + D_2O atmospheres.

The sintered body sample was polished with abrasive paper 1000 # (model). After polishing, the sample had a diameter of about 7.5 mm and a thickness of about 0.7 mm. Thereafter, a Pt paste was applied as an electrode and baked at 1000 °C for 1 h in an air atmosphere. Fig. 2 shows a schematic diagram of the experimental equipment used in this study. A Pt foil and a Pt lead wire were brought into close contact with the Pt paste applied to the surface of the sample, and the conditions were measured at an applied voltage of 1.0 V. The atmosphere was measured with Ar, Ar + H_2O, Ar + D_2O, and O_2. All the flow rates were 100 mL/min, and the temperature was measured from 1000 °C to 100 °C by decreasing the temperature every 100 °C. The conductivity σ (S/m) was calculated from the current value when a voltage was applied to the sample and it became steady.
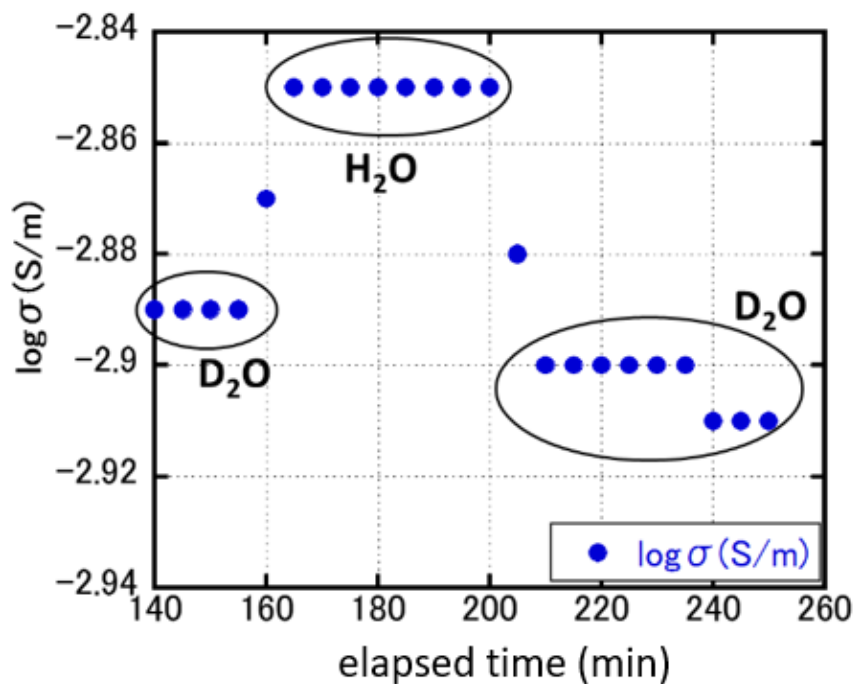
Fig. 5. Conductivity when the atmosphere changes between Ar + H_2O and Ar + D_2O at 1000 ° C.
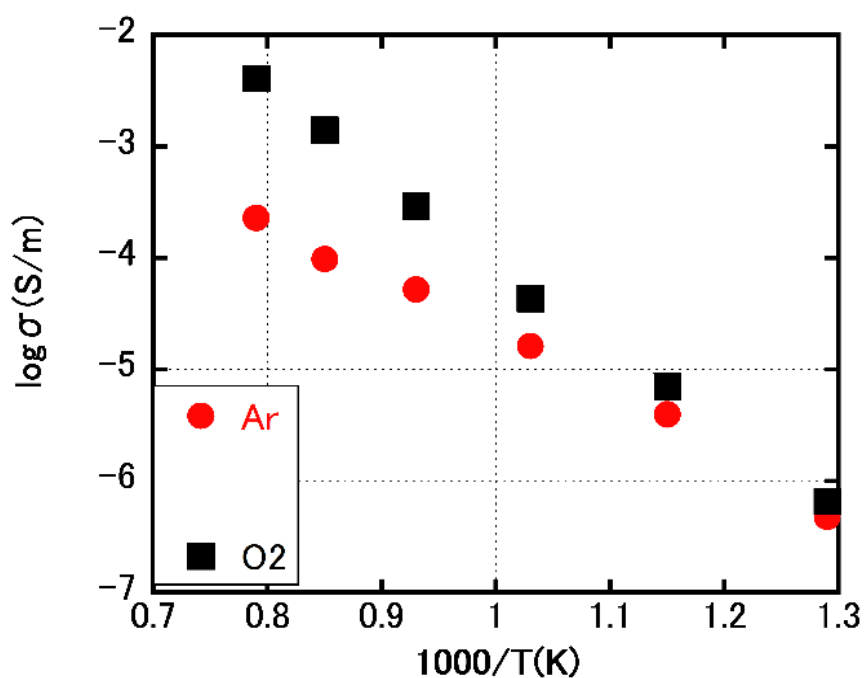

Fig. 6. Arrhenius plot of conductivity in Ar, and O_2 atmospheres.

3. RESULTS AND DISCUSSION

### 3.1 Identification of the sample crystal phase by XRD

Fig. 3 shows the XRD results of gadolinia in powder and sintered bodies. From this result, it was confirmed that the powder was cubic, but the crystal structure of the sintered body was changed to monoclinic. From the result of Archimedes' method, the density of the sintered body sample was 95% of the theoretical density.

### 3.2 Conductivity measurement of gadolinia

Fig. 4 shows an Arrhenius plot of conductivity measured in an atmosphere of Ar, Ar + H_2O, and Ar + D_2O. Increased conductivity was observed in Ar + H_2O and Ar + D_2O atmospheres compared to the Ar atmosphere.

Fig. 5 shows the atmosphere in which Ar + H_2O and Ar + D_2O atmospheres were exchanged at 1000 °C during measurement. Compared with Ar + H_2O, a decrease in conductivity was confirmed with Ar + D_2O. In addition, the conductivity of Ar + D_2O was lower than that of Ar + H_2O at all measured temperatures. This is due to the isotope effect, gadolinia is a proton conductor, and the reaction mechanism in the water vapor atmosphere follows Eq. (1) [16],

$$H_2O + O_o^\times + V_o^{\cdot\cdot} \leftrightarrow 2OH_o^{\cdot} \qquad (1)$$
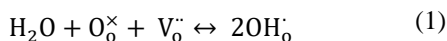
However, this conductivity difference became smaller as the measurement temperature was lowered. This suggests that the diffusion mechanism changes at low temperatures. Compared with the conductivity of $CaCe_{0.9}In_{0.1}O_3$ having a $CaZrO_3$ structure showing proton conductivity and the conductivity was about two orders of magnitude lower in a hydrogen atmosphere [13,17].

Fig. 6 shows an Arrhenius plot of conductivity measured in an Ar, O_2 atmosphere. In the O_2 atmosphere compared to the Ar atmosphere, the conductivity increased, and the higher the temperature, the higher the conductivity. This is thought to be due to hole conduction, and the reaction mechanism in the oxygen atmosphere is considered to follow Eq. (2) [18],

$$O_2 + 2V_o'' \leftrightarrow 2O_o^\times + 4h^{\cdot} \qquad (2)$$
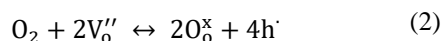
4. CONCLUSIONS

The conductivity was measured in an Ar, Ar + H_2O, Ar + D_2O, and O_2 atmosphere. A comparison of conductivity in Ar, Ar + H_2O, and Ar + D_2O atmospheres show that the conductivity of Ar + H_2O is higher than Ar + D_2O atmospheres are. Also, the Ar + D_2O atmosphere's conductivity was lower than that of the Ar + H_2O atmosphere. Besides, isotope dependence in the conductivity was observed, especially at high temperatures in the steam-containing atmospheres. This suggests that Gd_2O_3 is a proton-conductive oxide following the Grotthus mechanism of proton transport [17,19].

5. ACKNOWLEDGEMENTS

6. REFERENCES

[1] T. Hibino, H. Iwahara, The Hydrogen Isotope Separation by the Steam Electrolysis Using the High Temperature-Type Protonic Conductor., Nippon KAGAKU KAISHI. (1994) 518–523. https://doi.org/10.1246/nikkashi.1994.518.

[2] K. Yamazaki, T. Oishi, Tritium Fuel System Assessment on Economics and CO 2 Emissions in DT Fusion Reactors, Fusion Sci. Technol. 60 (2011) 1109–1112. https://doi.org/10.13182/FST11-A12609.

[3] K. Katayama, M. Nishikawa, Safety Confinement System, in: Tritium Fuel Fusion React., Springer Japan, Tokyo, 2017: pp. 297–329. https://doi.org/10.1007/978-4-431-56460-7_14.

[4] C.W. Forsberg, D.M. Carpenter, D.G. Whyte, R. Scarlat, L. Wei, Tritium Control and Capture in Salt-Cooled Fission and Fusion Reactors, Fusion Sci. Technol. 71 (2017) 584–589.

[5] V. Nemanič, Hydrogen permeation barriers: Basic requirements, materials selection, deposition methods, and quality evaluation, Nucl. Mater. Energy. 19 (2019) 451–457. https://doi.org/10.1016/j.nme.2019.04.001.

[6] T. Chikada, A. Suzuki, T. Kobayashi, H. Maier, T. Terai, T. Muroga, Microstructure change and deuterium permeation behavior of erbium oxide coating, J. Nucl. Mater. 417 (2011) 1241–1244. https://doi.org/10.1016/j.jnucmat.2010.12.283.

[7] T. Chikada, T. Tanaka, K. Yuyama, Y. Uemura, S. Sakurada, H. Fujita, X.-C. Li, K. Isobe, T. Hayashi, Y. Oya, Crystallization and deuterium permeation behaviors of yttrium oxide coating prepared by metal organic decomposition, Nucl. Mater. Energy. 9 (2016) 529–534. https://doi.org/10.1016/j.nme.2016.06.009.

[8] Y. Kawamura, S. Konishi, M. Nishi, Extraction of Hydrogen from Water Vapor by Hydrogen Pump Using Ceramic Protonic Conductor, Fusion Sci. Technol. 45 (2004) 33–40. https://doi.org/10.13182/FST04-A423.

[9] A. Ciampichetti, F.S. Nitti, A. Aiello, I. Ricapito, K. Liger, D. Demange, L. Sedano, C. Moreno, M. Succi, Conceptual design of Tritium Extraction System for the European HCPB Test Blanket Module, Fusion Eng. Des. 87 (2012) 620–624. https://doi.org/10.1016/j.fusengdes.2012.01.047.

[10] H. Iwahara, Recent trends of studies on proton conducting solid electrolytes, Electrochemistry. 69 (2001) 788–793. https://doi.org/10.5796/electrochemistry.69.788.

[11] M.K. Hossain, K. Hashizume, S. Jo, K. Kawaguchi, Y. Hatano, Hydrogen Isotope Dissolution Release Behavior of Rare Earth Oxides, Fusion Sci. Technol. 76 (2020) 553–566. https://doi.org/10.1080/15361055.2020.1728173.

[12] W. Mao, T. Chikada, A. Suzuki, T. Terai, H. Matsuzaki, Hydrogen isotope dissolution, diffusion, and permeation in Er 2 O 3, J. Power Sources. 303 (2016) 168–174. https://doi.org/10.1016/j.jpowsour.2015.10.091.

[13] H. IWAHARA, T. HIBINO, T. YAJIMA, Studies on Proton Conducting Ceramics Based on Perovskite-type Oxides., Nippon KAGAKU KAISHI. (1993) 1003–1011. https://doi.org/10.1246/nikkashi.1993.1003.

[14] M.K. Hossain, H. Tamura, K. Hashizume, Visualization of hydrogen isotope distribution in yttrium and cobalt doped barium zirconates, J. Nucl. Mater. 538 (2020) 152207. https://doi.org/10.1016/j.jnucmat.2020.152207.

[15] M.K. Hossain, K. Hashizume, Preparation and Characterization of Yttrium Doped Barium-Zirconates at High Temperature Sintering, in: Int. Exch. Innov. Conf. Eng. Sci., Fukuoka, Japan, 2020: pp. 70–72. https://doi.org/10.15017/2552940.

[16] N. Bonanos, A. Huijser, F.W. Poulsen, H/D isotope effects in high temperature proton conductors, Solid State Ionics. 275 (2015) 9–13. https://doi.org/10.1016/j.ssi.2015.03.028.

[17] C.J.T. de Grotthuss, Memoir on the decomposition of water and of the bodies that it holds in solution

by means of galvanic electricity, Biochim. Biophys. Acta - Bioenerg. 1757 (2006) 871–875. https://doi.org/10.1016/j.bbabio.2006.07.004.

[18] G.V.S. Rao, S. Ramdas, P.N. Mehrotra, C.N.R. Rao, Electrical Transport in Rare-Earth Oxides, in: 1995: pp. 347–354. https://doi.org/10.1142/9789812795892_0028.

[19] K.-D. Kreuer, Proton Conductivity: Materials and Applications, Chem. Mater. 8 (1996) 610–641. https://doi.org/10.1021/cm950192a.